

Egyptian Journal of Chemistry

http://ejchem.journals.ekb.eg/



Corrosion Inhibition of Monel 400 in 1M HCl Using a Novel Eco Inhibitor Curcumin and Bis Curcumin Bis Azodye



Mahmoud Abbas¹, Reda M.Abd El-Aal², Amira M. Beshta*³ and Dalia M. Abbas⁴

^{1,3}Suez University, Faculty of IPetroleum and Mining Engineering, Metallurgical and Material Engineering.

²Suez University, Faculty of Sci., Chemistry Department, 4Egyptian petroleum Research institute, Egypt

Abstract

Corrosion inhibition of Monel 400 in 1M HCl using new synthesis environmentally friendly compound bis curcumin bis azodye (BCBAD) was studied. BCBAD was prepared via diazotization of p-phenylenediamine and coupling bimolar ratio of 1,7-bis(4-hydroxy-3-methoxyphenyl)-1,6-heptadiene-3,5-dione (curcumin). Structure of the new dye BCBAD was checked and confirmed by Nuclear Magnetic Resonance (1H-NMR), Fourier-Transformer Infrared (FTIR) spectroscopy and Mass-spectrum. Potentiodynamic polarization and cyclic polarization Techniques were carried out to evaluated effect of curcumin and BCBAD on the electrochemical behaviour of Monel 400. Samples with different concentrations of 25,50,100,150 and 200 ppm in 1M of HCl were studied. Results showed that corrosion rate of blank was 18.576 mpy, curcumin with the best concentration 150 ppm was 4.51mpy with 76% efficiency and the best concentration 200 ppm of BCBAD was 0.957mpy with 95% efficiency. Thus, BCBAD was performed as an excellent inhibitor. The protective layer formed by curcumin consists mainly of Cu(OH)₂·H₂O, with an average thickness of 27.33 µm and average protective layer thickness which consisted of Fe2N and CuO using BCBAD was 44.13µm. Adhesion of curcumin was classified according to ASTM D3359 method B was (1B) where BCBAD was (3B).

Keywords: Electrochemical; Curcumin; Azodye; Monel 400.

1. Introduction

Monel 400 is one of the most important nickel-based alloys with copper, 3% iron, traces of manganese and silicon, it is used in petrochemicals, chemical industries, heat exchanger, pumps and many others applications, it has high strength actoughness comparable to structural steel, it has good corrosion resistant in chloride and stress corrosion cracking in typical environments [1]. When Monel 400 exposed to stagnant chloride solution corrosion has been observed. Therefore, the useful methods to prevent or minimize pitting corrosion is the addition of inhibitors. However, most inhibitors are toxic or harmful to the environment and costly so organic compounds inhibitors containing oxygen, nitrogen and hydrogen can be used, they have active adsorption on metal surfaces [2-4]. Curcumin and curcumin extraction could be used as a preferred alternative to inorganic chemicals. It was found that the inhibition efficiency depends on the adsorption of curcumin and its derivatives particles on Monel surface to form a protective layer against corrosion agents leads to increases the resistance to corrosion [5]. Toxicity and environmental properties of selected inhibitors depend on their chemical composition. Common inhibitors like chromates are highly toxic and carcinogenic and have posing risks to human health and ecosystems. Organic inhibitors (e.g., benzotriazole) are less toxic but may still be harmful if not biodegradable. Green inhibitors (e.g., plant extracts) are ecofriendly, non-toxic, and biodegradable, making them preferable for sustainable applications [6].

Recent studies have demonstrated their significant potential as effective corrosion inhibitors, particularly in acidic environments. It is important to highlight that the majority of existing studies have primarily focused on copper, stainless steel and carbon steel in acidic corrosive media [7,8]. A little attention has been made to investigate the effect of curcumin and bis curcumin bis azodye (BCBAD) on the corrosion behavior of Monel 400 alloy in acidic environment. Therefore, the objective of the present study is to investigate the inhibition effect of curcumin and BCBAD on electrochemical behavior and corrosion of Monel 400 in 1.0 M HCl solution by potentiodynamic polarization and cyclic polarization.

While previous studies have demonstrated the effectiveness of natural plant extracts as eco-friendly corrosion inhibitors for conventional metals - such as Aloe ferox Mill extract achieving 93.3% efficiency for copper in 1.0 M HCl through physisorption [9]. Outperforming Schiff base inhibitors at 250 ppm gave 93% efficiency [10]. The modified curcumin derivative formed a 44.13 µm protective layer - 61.5% thicker than pure curcumin (27.33 µm) - with enhanced adhesion (3B vs. 1B, ASTM D3359). This structural modification through azo-group incorporation significantly improves both electrochemical performance and interfacial stability while maintaining environmental advantages over synthetic inhibitors, aligning with emerging trends in green corrosion protection. [11]. These approaches remain limited by thermal instability and restricted alloy compatibility. The present study advances the field by developing bis-curcumin bis-azodye (BCBAD), a

*Corresponding author e-mail: <u>amiram2427@gmail.com</u>.; (Amira M Bestha).

Received date 15 July 2025; Revised date 04 September 2025; Accepted date 09 September 2025

DOI: 10.21608/ejchem.2025.404494.12051

©2026 National Information and Documentation Center (NIDOC)

synthetic derivative that addresses these limitations for Monel 400, a technologically critical Ni-Cu alloy in petrochemical and marine applications. BCBAD exhibits superior performance (94.8% efficiency at 200 ppm) compared to both pure curcumin (75.7%) and reported plant extracts, while forming a 44.13 μm protective layer - 61.5% thicker than natural curcumin's 27.33 μm layer - with exceptional adhesion (ASTM 3B vs 1B). Electrochemical and surface characterization (SEM, EDX, XRD) confirms BCBAD's mixed chemisorption-physisorption mechanism, involving Fe₂ N/CuO formation, which outperforms the purely physisorption behavior of natural compounds can enhance both performance metrics (efficiency, layer durability) and industrial applicability for advanced alloys under aggressive conditions.

2.1 Experimental

2.1 Materials

All the purchased chemicals were used without any further purification. Monel 400 was supplied from Suez Oil Processing Company (SOPC) in Suez, Egypt. It is used as metallic materials with chemical composition as described in the Tables 1,2. P-phenylenediamine, dimethylformamide (DMF), NaOH, HCl, NaNO₂ and curcumin were purchased from (Sigma Aldrich, >99.5 wt %). Fourier Transform Infrared (FTIR) spectra were obtained using a Pye Unicame-1200 spectrometer with potassium bromide (KBr) discs. UV-visible (UV-Vis) spectra were recorded on a Jasco V-550 spectrophotometer (Faculty of Science, Suez University). Nuclear Magnetic Resonance (1H-NMR) analysis of the new synthesized azodye compounds was performed on a Bruker ECZ Luminous (JNM-ECZL series) 500 MHz spectrometer at the National Research Centre. Samples were prepared by dissolving the compounds in dimethyl sulfoxide (DMSO). Mass spectrometry of the synthesized compounds was carried out at the Regional Center for Mycology and Biotechnology, Al Azhar University.

Table 1: Chemical composition of Monel 400 using XRF in SOPC

Ni (wt%)	Cu (wt%)	Fe (wt%)	Si (wt%)	Mn (wt%)	Al (wt%)	S (wt%)	Ti (wt%)
62.52	31.95	2.14	1.34	0.931	0.526	0.526	0.044

Table 2: Mechanical properties of Monel 400 [12]

Tensile Strength, yield	Tensile Strength, Ultimate	Elongation at Break
240 MPa	550 MPa	40 %

Surface morphology and elemental composition were investigated using various techniques: Scanning Electron Microscopy (SEM) with JEOL instrument, Energy-Dispersive X-ray spectroscopy (EDX) with Quanta at FEG 250 instrument, X-ray Diffraction (XRD) with a Panalytical X'Pert Pro NC 4022 diffractometer. Synthesis of bis-[1,7-bis(4-hydroxy-3-methoxyphenyl)-1,6-heptadiene-3,5-dione-4,4--bisazodye-1-,7--bis(4--hydroxy-3-methoxyphenyl)]-1-,6--heptadiene-3,5-dione (curcumin) bimolar ratio with an one molar ratio of p-phenylenediamine diazonium salt in acid solution (HCl) [13,14]. An amount of 0.02 moles of p-phenylenediamine was dissolved in 15 ml of concentrated hydrochloric acid, cooled to 0-5°C, diazotized with 0.04 moles of sodium nitrite dissolved in 5 ml of distilled water. After 20 min the diazonium solution was slowly added to a solution of 0.02 moles of 1,7-bis(4-hydroxy-3-methoxy-phenyl)-1,6-heptadiene-3,5-dione (curcumin) containing 5 g of sodium carbonate and 50 ml of water also cooled to 5°C. After 2h, buffering the mixture with sodium acetate (1:4) was added until the solution was slightly acidic (PH 5–6), Scheme 1. The bis curcumin bis azodye (BCBAD) separated as a dark red precipitate which was filtered off and washed several times with water was purified by recrystallization from hot ethanol, m.p. = 177-2 °C, (Yield 87.7%), Mol. form. C48H42N4O12, Mol. Wt. = 866 and Mass-spectrum reveals M+1= 867.

$$\begin{array}{c|c} H_2N & & & \\ \hline & NH_2 & & \\ \hline & 1 & \\ \hline & 1 & \\ \hline & & \\ \hline & 1 & \\ \hline & & \\ \hline &$$

Scheme 1: Synthesis of bis curcumin-bis azodye (BCBAD)

The structure of Synthesis of bis curcumin-bis azodye (BCBAD) as showed in Scheme 1, was confirmed by IR spectroscopy, ¹H-

2.2 Preparation of Specimen

NMR, and Mass spectrum Fig. 1-3, respectively.

Monel samples were sectioned into $1 \times 1 \times 0.5$ cm coupons for electrochemical testing. The preparation protocol included Degreasing: Ultrasonic cleaning in acetone for 10 minutes followed by air-drying, Mounting: Encapsulation in two-part epoxy resin ,within glass holders, Electrical contact: Attachment of insulated copper wires to the specimen backs using conductive silver epoxy and Surface finishing (Wet grinding with 1200-grit Sic paper under deionized water cooling, Rinsing with absolute ethanol (99.8%), Final air-drying under nitrogen stream) [15].

2.3 Making of test solution

For each chemical, a standard stock solution was made by 1 liter of distillated water & 1M of HCl solution, the concentrations of the inhibitor stock solution changed to suit the demands of the experiment, in between $50 \rightarrow 200$ ppm.

2.4. Electrochemical Testing

2.4.1 Potentiodynamic polarization

Electrochemical experiments were performed using a VoltaLab-PGZ100 potentiostat (Radiometer Analytical) interfaced with a personal computer and controlled by VoltaMaster-4 software (version 7.08). A conventional three-electrode electrochemical cell was configured with:

- Working electrode (WE): Pretreated Monel 400 coupon (1 cm² exposed area)
- Counter electrode (CE): Platinum mesh (2 cm²)
- Reference electrode (RE): Saturated Calomel Electrode (SCE)

Following Open Circuit Potential (OCP) reached the steady state, measurements were carried out, using a sweep rate of 12 mv/s, and the initial and final potential were (-1,1) V, OCP. Corrosion Rate, (C.R), The corrosion current density (i_{aorr}) was determined by extrapolating the linear Tafel segment of the cathodic polarization curve to the corrosion potential Ecorr. The inhibition efficiency (IEp%) was estimated from the change in corrosion Rate (C.R), as per Eq. (1)

$$IE\% = [C.Ro - C.Ri / C.Ro] 100$$
 Eq. (1)

Where C.Ro and C.Ri are the Corrosion Rate of Monel 400 in uninhibited and inhibited solutions, respectively.

2.4.2 Cyclic polarization

To determine pitting potential of the specimen's tests were operated in 1M HCl solution from an initial potential of -2V with respect to OCP to a final potential of -2V with respect to the Saturated Calomel Electrode keeping the vertex potential to be -2V with scan rate of 3mV.S-1 and the corresponding current was recorded. In other method, the specimens were submerged in the Corroding solution for about 3 weeks are shown in Fig. 10 and 11 for curcumin and BCBAD respectively.

2.4.3 Surface morphology analysis

The Monel specimens were readied for surface morphology examination, following the procedure outlined in the comparison of conditions with and without the inhibitor. The polished specimens were immersed for 21 day in 1 M HCl medium, either without or with the curcumin and BCBAD concentration. Following rinsing with water and subsequent drying, the corroded specimens were analyzed using a Dimension ICON AFM equipped with Scan Asyst. Optical microscopy after specimens' preparation, macro structural examination was carried out using the optical microscope at meg. From 5x to 50X by Olympus BX41M- LED.

A) X-Ray Diffraction (XRD)

The Monel samples were prepared for surface morphology analysis as described. Using (Bruker D8 Discover Model) is using by wide Angle X-ray Diffraction with Small Angle Capability.

B) EDX Analysis

Using JEOL electron microscope (Standard on IT500/IT700/IT800 series) Atomic Energy Authority(Gamma Radiation Center).

C) Thickness layer

The specimens of Monel 400 with 150 ppm curcumin and 200 ppm BCBAD were immersed in 1M HCl for 21 days, pour the mounting in a vertical position after specimens come out the solution. The samples were photographed and the thickness of the layer formed was determined by optical microscope Olympus BX41M- LED.

2.4.4 Adhesion Test

The adhesion test was done with the tap adhesion test (X-cut) ASTM D3359. This test method describes how to measure how well coating films stick to metal substrates by putting pressure- sensitive tape over cuts in the film and then removing it.

3. Results and Discussion

1ST BCBAD inhibitor

3.1 (FT-IR) Spectra:

FT-IR spectra of compound bis curcumin bis azodyes (2), Fig.1 shows the function groups of compound (2) by FT-IR. It could be noted that absorption peak at 600-800 cm⁻¹ to benzene rings, at 1200-1300 cm⁻¹ for O-CH3, at 1600 cm⁻¹ for C=C, at 1620 cm⁻¹ for C=O, broad peak at 3400-3500 cm⁻¹ for -OH groups, at 1423 cm⁻¹ for N= N, at 1580 cm⁻¹ for conjugated C=C and at 1584 cm⁻¹ for C=O.

3.1.1 1H-NMR (DMSO- δ ppm) and Mass-Spectrum:

Fig.2 show the 1 H-NMR for compound (2) reveals signals at δ ppm = 7.10-7.95 (m, 16H, Ar-H), 6.55-6.85 (dd, 8H, 4CH=CH group), 5.51(s, 4H, 4-OH groups), 4.65 (s, 2H, two CH) and at δ 2.85(s, 12H, 4-O-CH3 group), Mass spectrum for compound (2) gives M+1= 867, Fig.3.

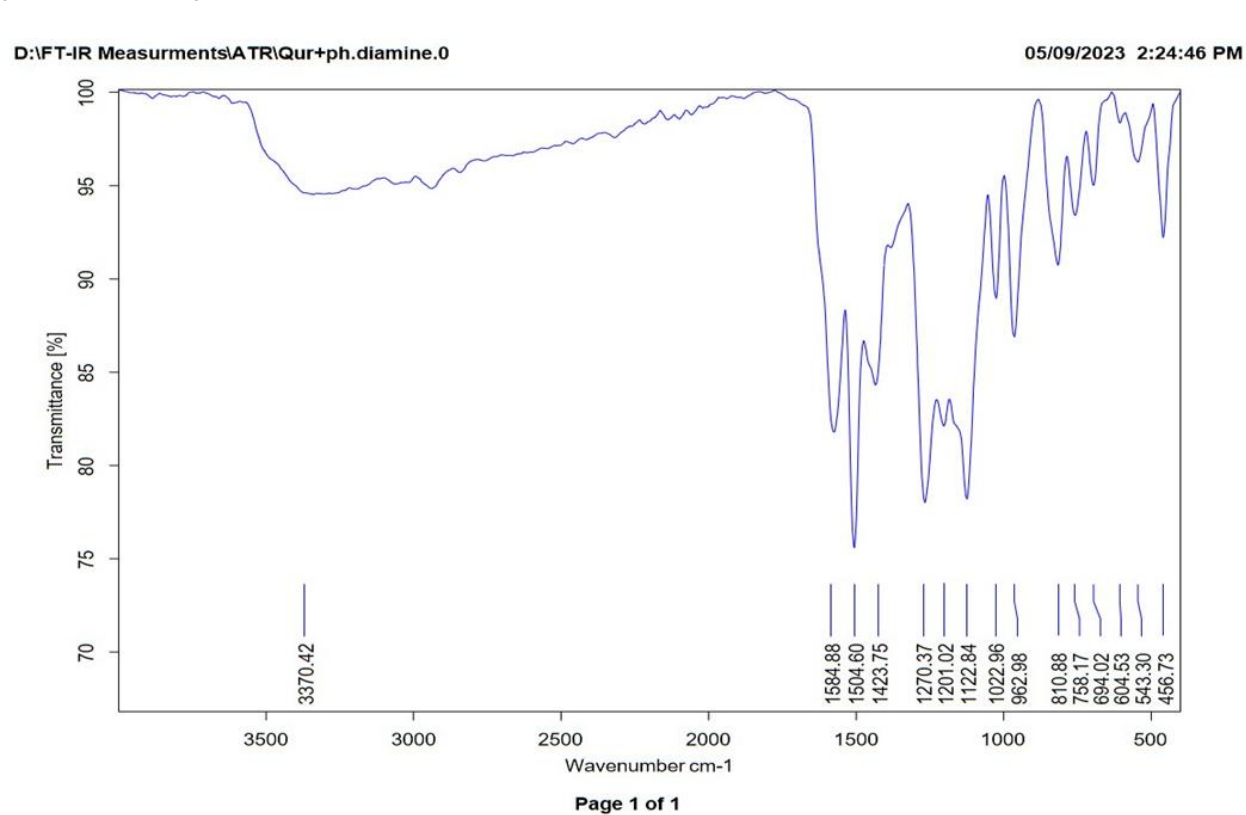


Figure 1: (FT-IR) spectrum of BCBAD

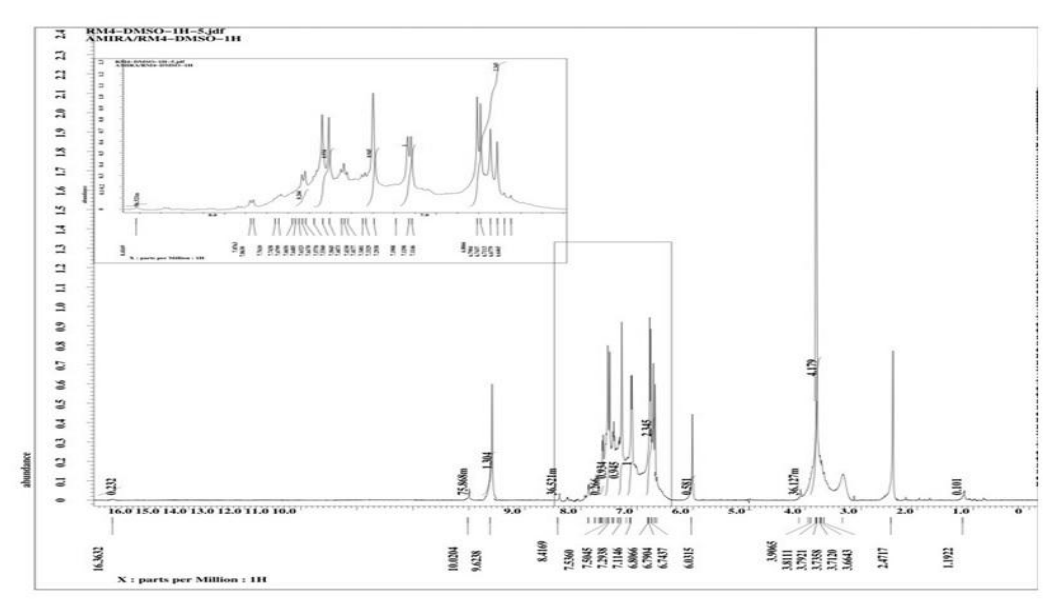


Figure 2: (1 H-NMR) spectrum of BCBAD

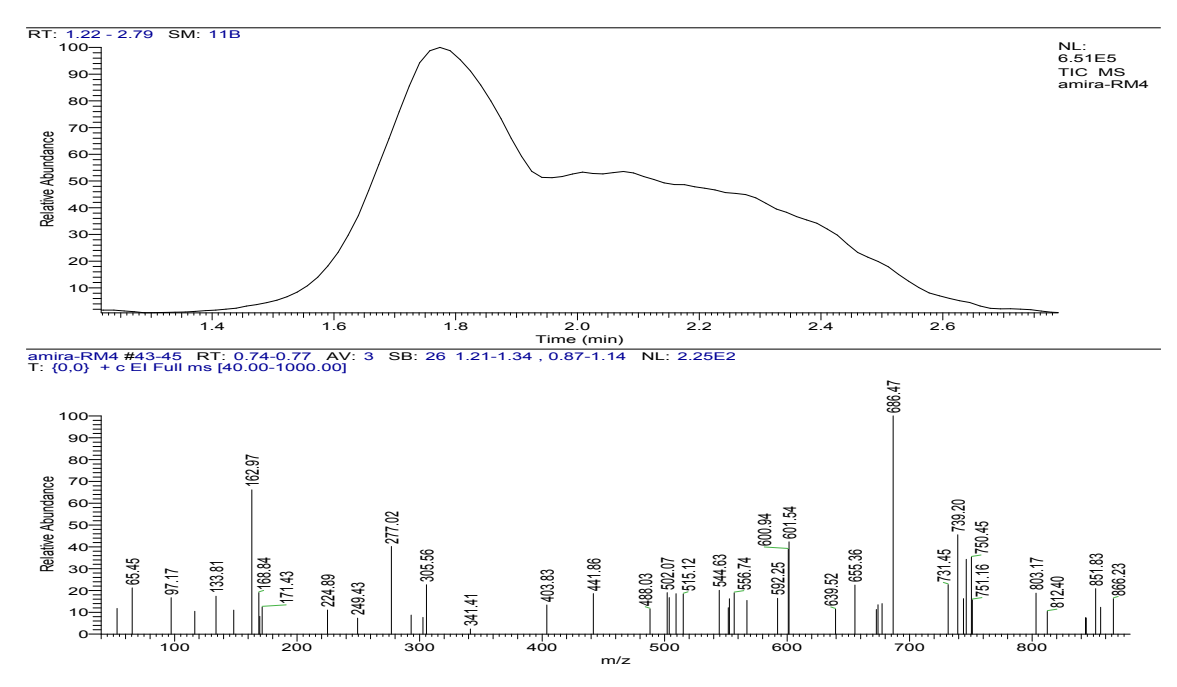


Figure 3: Mass Spectrum of BCBAD

3.2 Electrochemical study

3.2.1 Potentiodynamic Polarization

Fig. 6 and 7 show the polarization curves applied to Monel 400 exposed to 1M HCl solution with different concentration at 25°c for curcumin and BCBAD, respectively. The polarization curves shifted to the left (lower current densities) with increasing inhibitor concentrations, indicating reduced metal dissolution in 1 M HCl. This effect was most pronounced at concentrations above 150 ppm for curcumin and 200 ppm for BCBAD, demonstrating optimal inhibition [16]. The active surface area exposed to the corrosive medium is reduced by the formation of a protective film on the metal, delaying both hydrogen evolution and metal dissolution. The coverage of inhibitor molecules on the surface is enhanced at higher concentrations up to 150 and 200 ppm for curcumin and BCBAD, respectively. Table 3 presents the electrochemical parameters derived from polarization curves for Monel 400 in 1 M HCl solution at 25°C, showing the effects of varying concentrations of curcumin and BCBAD inhibitors. It was found that Fig.8 a,b shows corrosion rate change of Monel 400 in 1M HCl for curcumin and BCBAD, respectively. While, Fig.9 a,b shows change of inhibition efficiency (IE) with curcumin and BCBAD, respectively. It could be observed that maximum inhibition efficiency 75.72% and 94.84% of curcumin and BCBAD, respectively. The corrosion inhibition performance of both compounds improves progressively with higher concentrations, reaching maximum values at 150 ppm for curcumin and 200 ppm for BCBAD.

Table 3: Potentiodynamic polarization results in the absence and presence of inhibitors for Monel 400 in 1M HCl solution at deference concentration at 25°C

Compd.	Conc.	Corrosion	Ecorr	Icorr	Ba (v/dec)	Bc (v/dec)	IEp (%)
сотра.	Conc.	rate (mpy)	(mv)	(μA/cm2)	Bu (videe)	Be (videe)	ILP (70)
Blank	0	18.576	429.543	40.972	.006615	0.1465	0
Curcumin	25	13.127	554.136	28.954	68.305	6.195	29.33
	50	11.73	651.9	25.827	0.00173	0.349	36.96
	100	8.1602	659.9	17.998	-6.663	0.5	56.07
	150	4.51	662.097	9.947	-461.237	-25.33	75.72
	200	14.397	557.51	31.754	0.0429	0.145	22.49
BCBAD	50	8.0922	682.655	17.848	0.3936	0.2768	56.43
	100	5.9755	755.029	13.18	-4.932	66.453	67.83
	150	2.4787	781.406	5.467	0.464	0.251	86.65
	200	0.95709	800.945	2.111	-0.307	.078	94.84
	250	13.616	661.484	30.032	3.841	0.923	26.70

3.2.2 Potentiodynamic Polarization for Curcumin

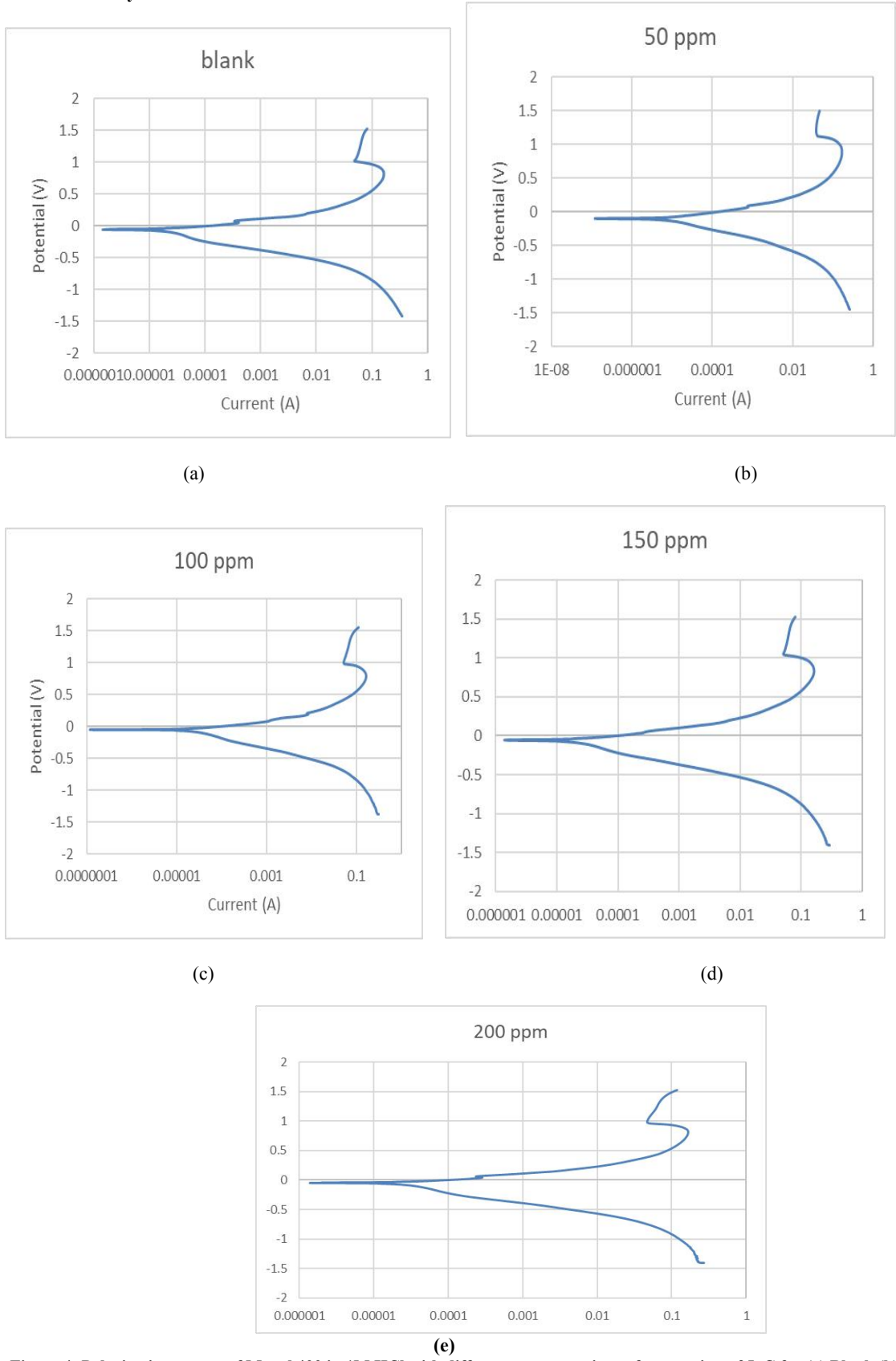


Figure 4: Polarization curves of Monel 400 in 1M HCl with different concentrations of curcumin at 25oC for (a) Blank (b) 50 ppm (c) 100 ppm (d) 150 ppm (e) 200 ppm

3.2.3 Potentiodynamic Polarization for BCBAD

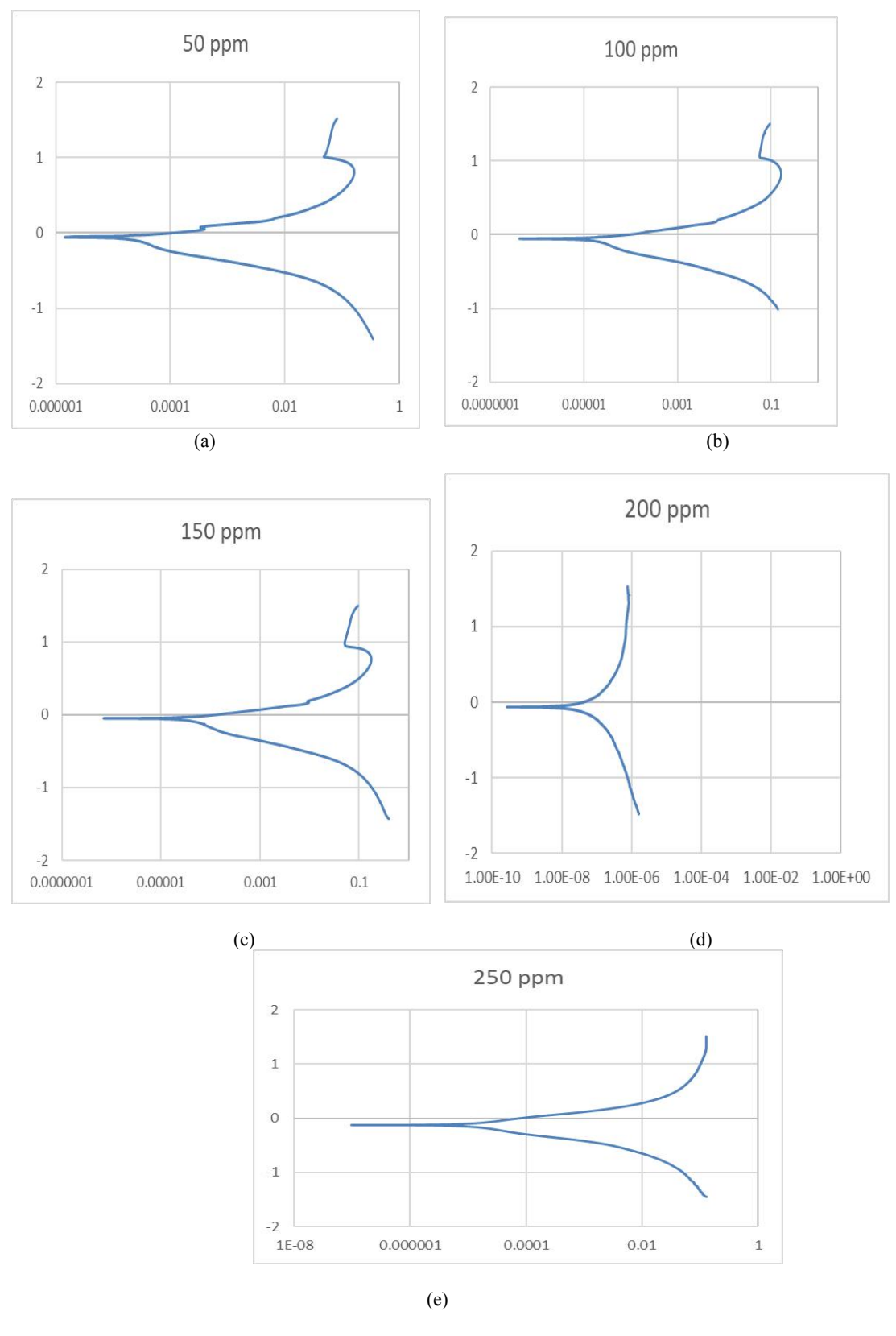


Figure 5: Polarization curves of Monel 400 in 1M HCl with different concentrations of BCBAD at 25oC for (a) 50 ppm (b) 100 ppm (c) 150 ppm (d) 200 ppm (e) 250 ppm

3.2.4 Mixed Potentiodynamic Polarization for Curcumin

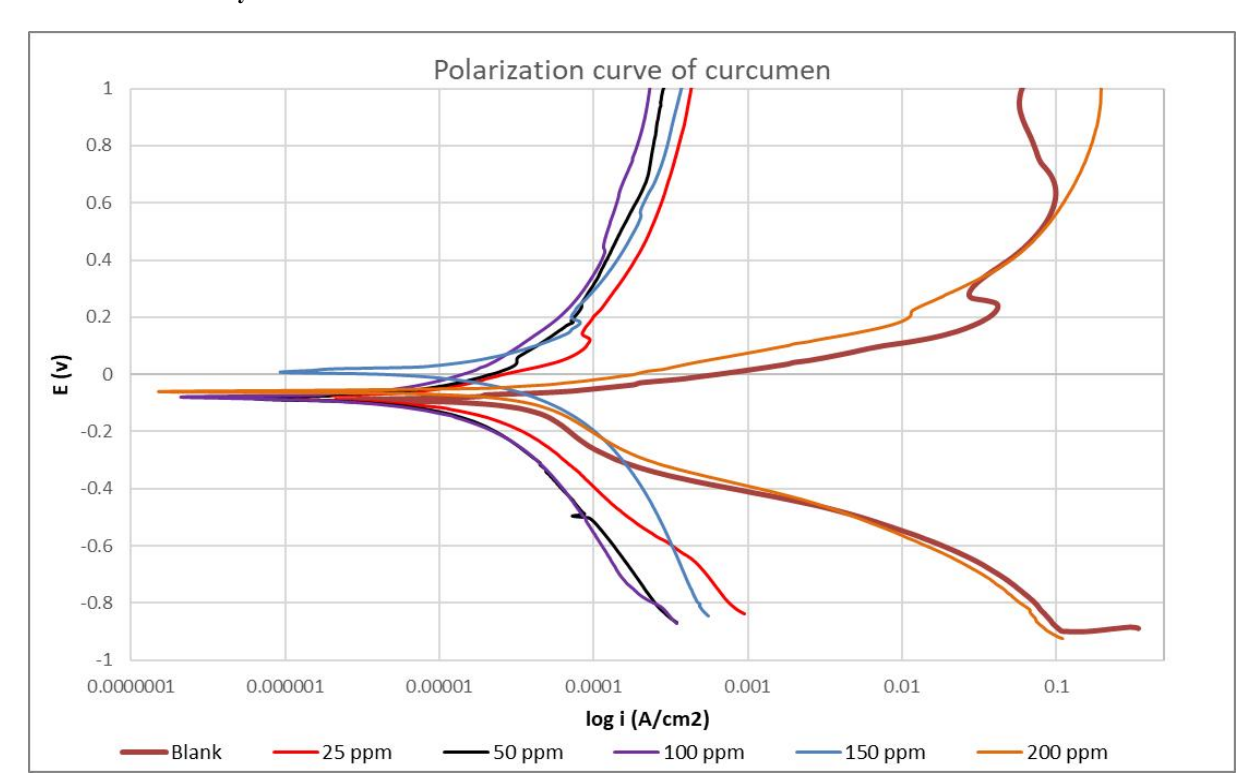


Figure 6: polarization curves of Monel 400 in 1M HCl solution with different concentrations of curcumin at 25°C.

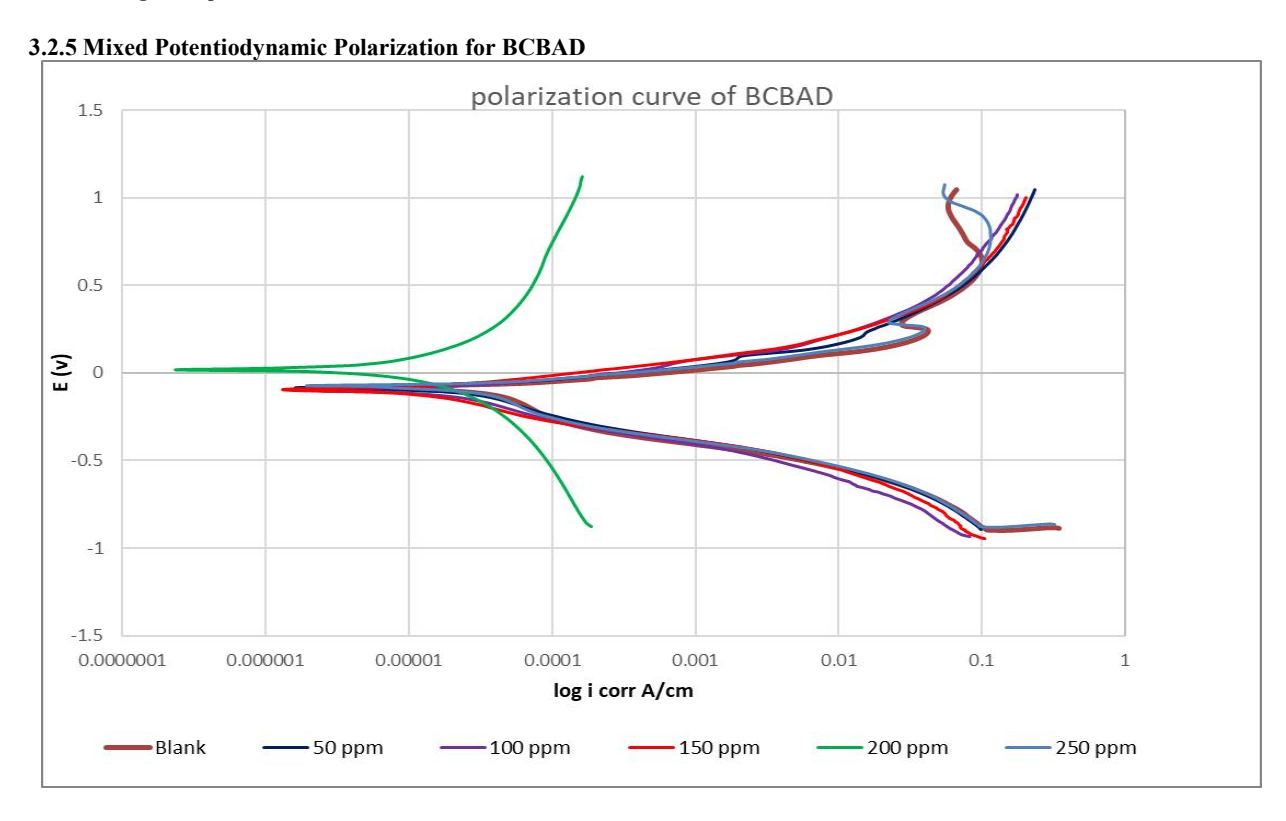
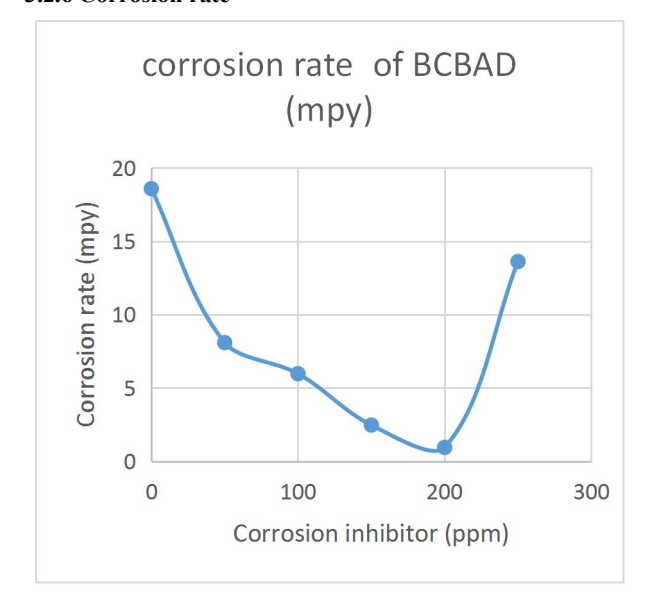
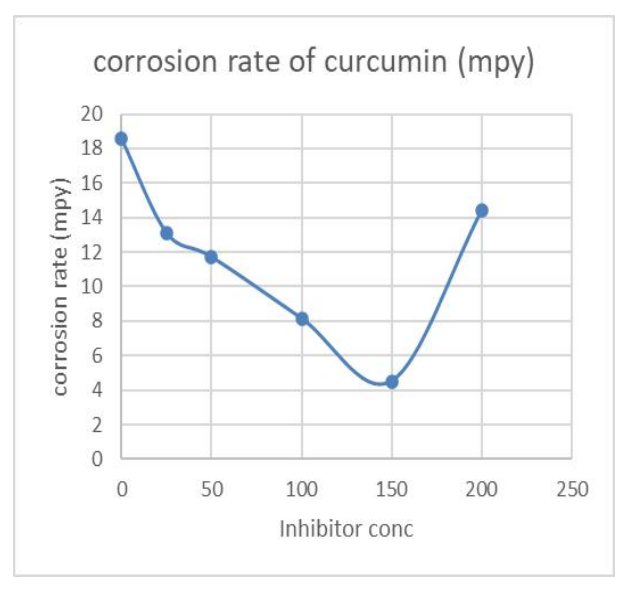


Figure 7: Polarization curve of Monel 400 in 1M HCl solution with different concentrations of BCBAD at 25°C

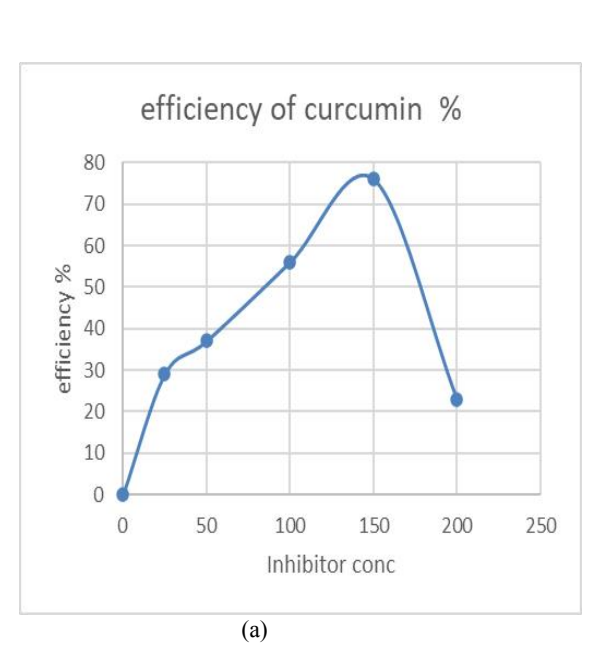
3.2.6 Corrosion rate





(a) (b) Figure 8: Corrosion rate of Monel 400 in 1M HCl with different concentrations at 25°C for (a) Curcumin (b) BCBAD

3.2.7 Efficiency



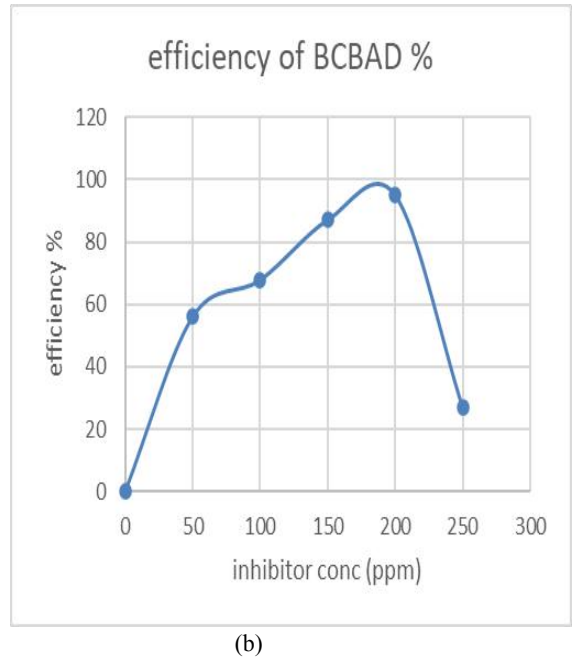
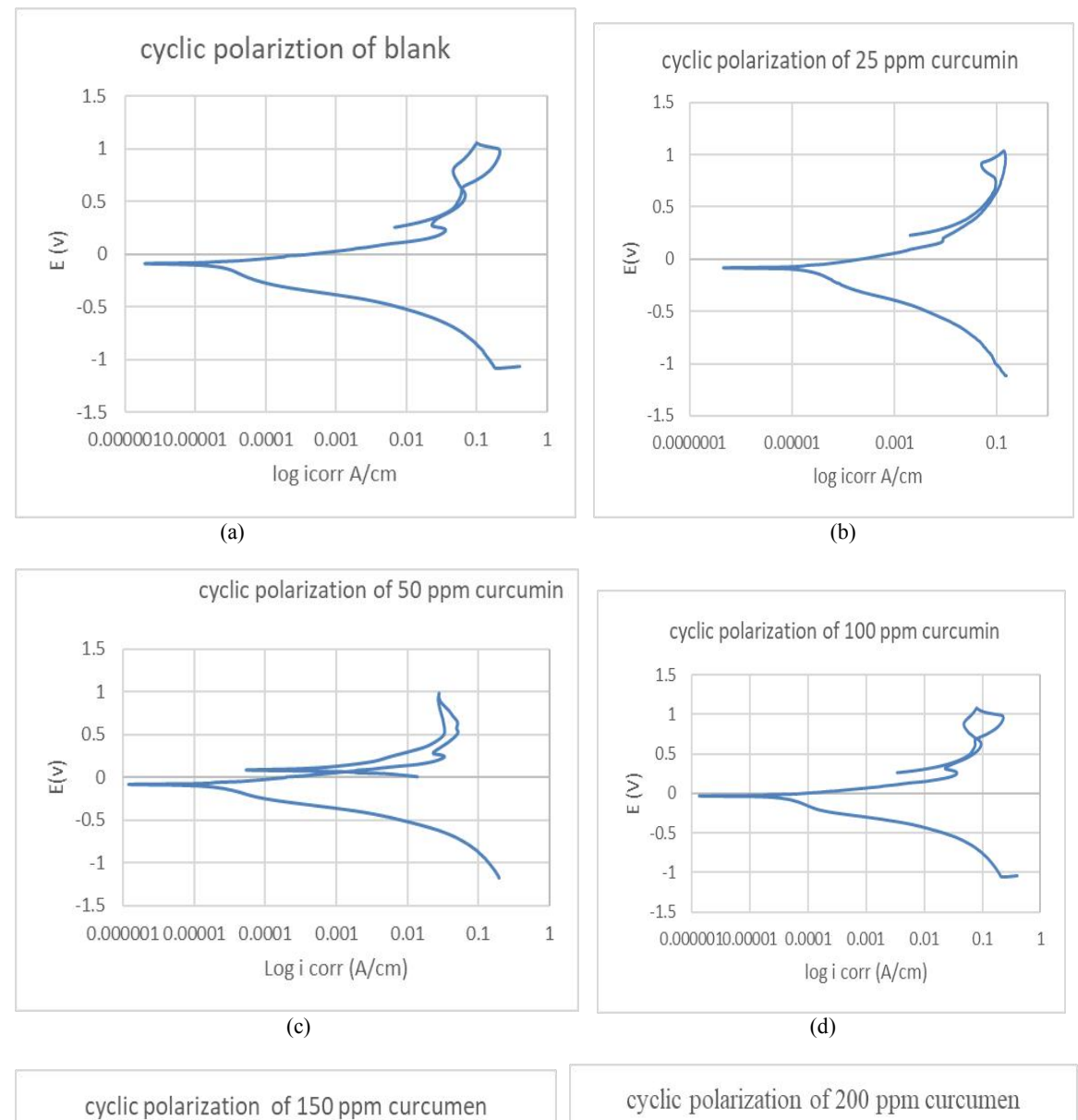


Figure 9: Efficiency (%) of Monel 400 in 1M HCl with different concentrations at 25°C for (a) Curcumin (b) BCBAD

3.2.8 Cyclic polarization

Cyclic polarization curves applied to Monel 400 exposed to 1M HCl without inhibitor, with curcumin and BCBAD are shown in Fig.10 a-f and Fig.11 a-e, respectively. It was observed that pitting potential increase with increasing either curcumin or BCBAD. Pitting potential of Monel 400 for curcumin and BCBAD are shown in Fig.12 a,b respectively. It increases from 429.543 to 800.945 with improvement of pitting potential 86.46% for 200 ppm BCBAD. This means more resistance to pitting corrosion.

A) Cyclic polarization of Curcumin



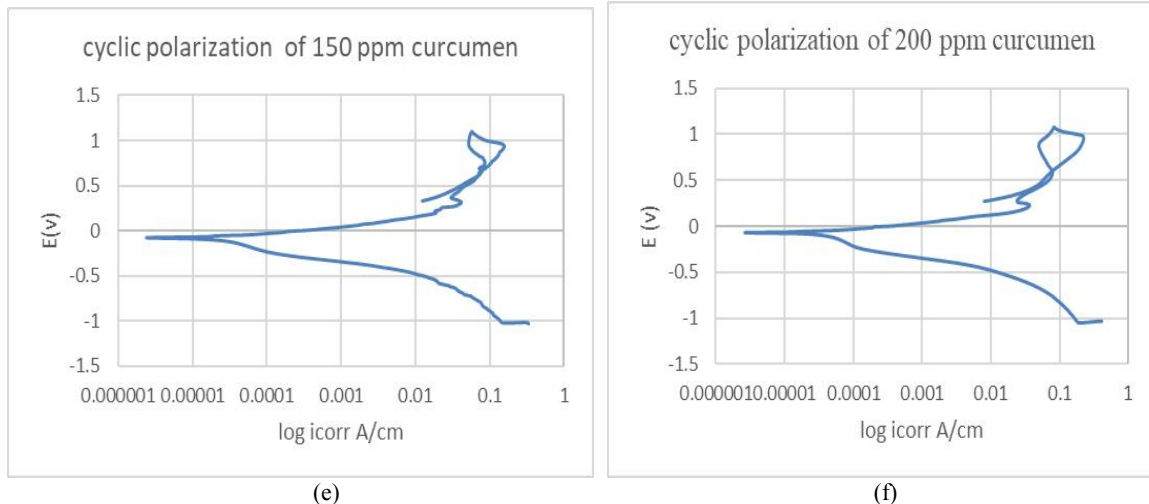


Figure 10: Cyclic polarization curve of Monel 400 for curcumin in 1M HCl solution at 25°C (a) blank (b) 25 ppm (b) 50 ppm (d) 100 ppm (e) 150 ppm (f) 200 ppm

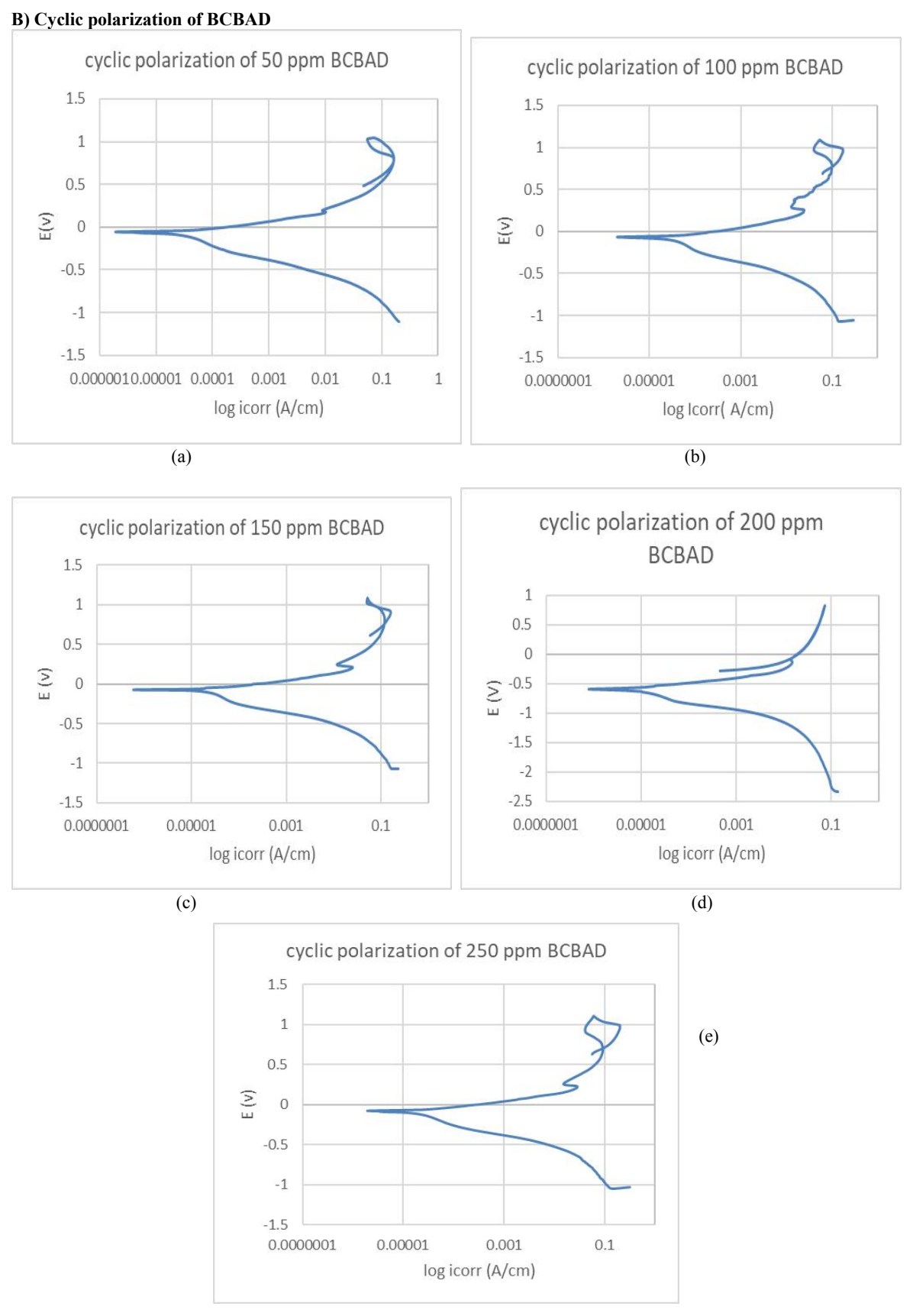


Figure 11: cyclic polarization of Monel 400 for BCBAD in 1M HCl solution at 25oC at (a) 50 ppm (b) 100 ppm (c) 150 ppm (d) 200 ppm (e) 250 ppm

3.2.9 Pitting Corrosion

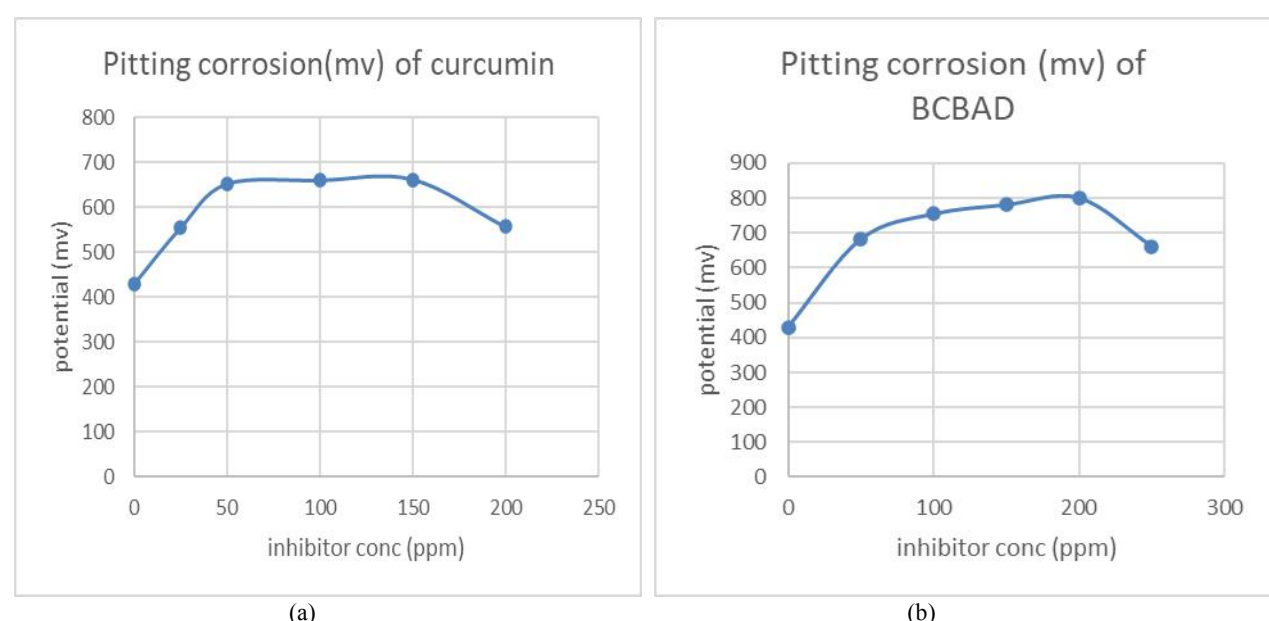


Figure 12: Pitting corrosion of Monel 400 in 1M HCl solution for different concentrations at 25 °C for (a) curcumin (b) BCBAD

Table 4: Comparison of pitting corrosion of Monel 400 for BCBAD, curcumin

Table it comparison of piving corrosion of filence too for Bobile, careamin				
Inhibitor concentration (ppm)	Pitting corrosion (mv)	Improvement of the pitting potential%		
Blank	429.50			
Curcumin (150 ppm)	662.00	54.13%		
BCBAD (200ppm)	800.95	86.46%		

3.4. Adhesion Test

Figure 13 a,b show that the result of adhesion test applied to Monel 400 exposed to 1M HCl with 150 ppm curcumin and 200 ppm BCBAD, respectively. The test carried out according to standard ASTM D3359 Method B. BCBAD was grad (3B) percent area removed (5-15%) small flakes of the film are detached at long edges and intersections of cuts the area affected 5% to 15% of the lattice where curcumin was classified as (1B) percent area removed (35-65%) the film has flaked along the edges of cuts in large ribbons whole squares have detached the area affected 35 to 65% of the lattice it could be observed that the film of BCBAD has better adhesion than curcumin due to the bonding force between the film and substrate.

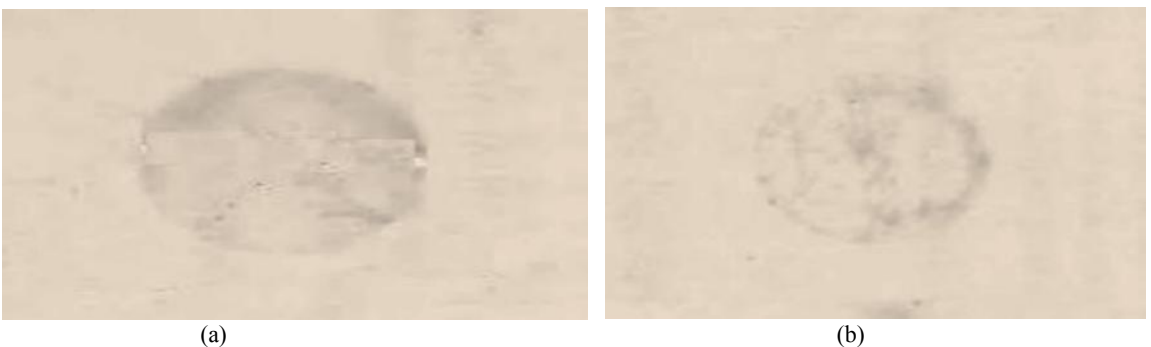


Figure 13: Adhesion test of Monel 400 in 1M HCl solution for a) 150 ppm Curcumin b) 200 ppm BCBAD

3.5. Thickness of layer

Figure 14 a,b shows that result of the thickness layer measurements of Monel 400 in 1M HCl curcumin and BCBAD where the thickness layer of curcumin $(27.33\mu m)$ and the thickness layer of BCBAD $(44.13\mu m)$. The layer of BCBAD is thicker than curcumin.

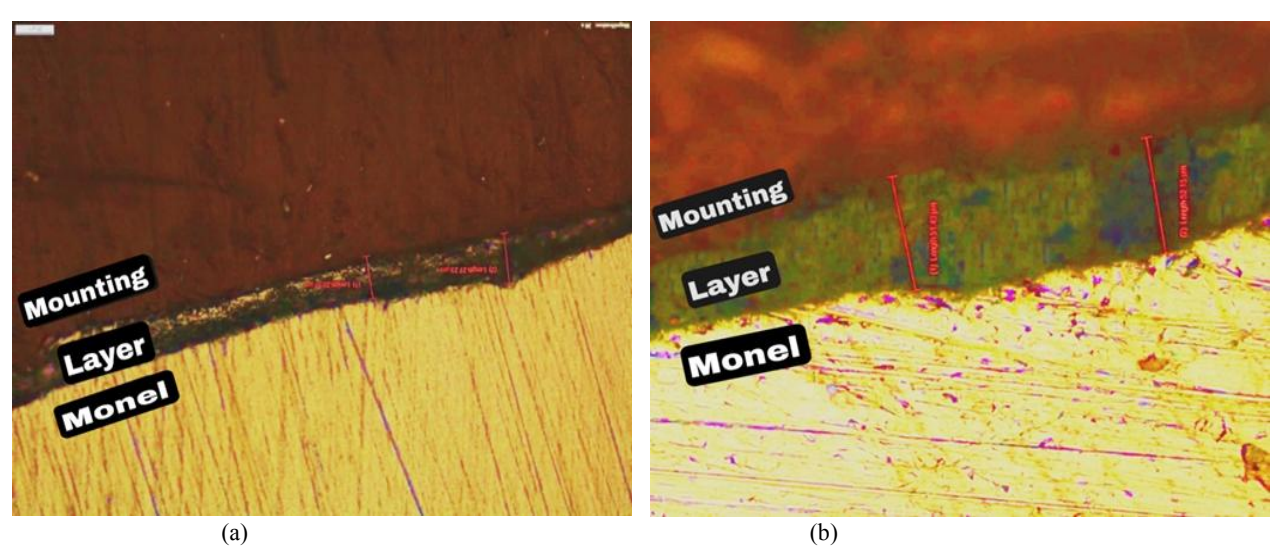


Figure 14: The thickness layer of Monel 400 in 1M HCl solution for a) curcumin (27.33µm) b) BCBAD (44.13µm)

3.6. Investigations (SEM, EDX, and XRD)

3.6.1. Scanning Electron Microscope (SEM)

Fig.15 a-c shows Scanning Electron Microscope of Monel 400 in 1M HCl for Blank (without inhibitor), 150 ppm curcumin and 200 ppm BCBAD. Fig. 16 a-c shows Microscope images of Monel 400 in 1M HCl for Blank (without inhibitor), 150 ppm curcumin and 200 ppm BCBAD, respectively. Analysis reveals no detectable corrosion products on metal surfaces in inhibited solutions, confirming the inhibitor film's effectiveness in preventing both oxidative dissolution and reduction reactions.

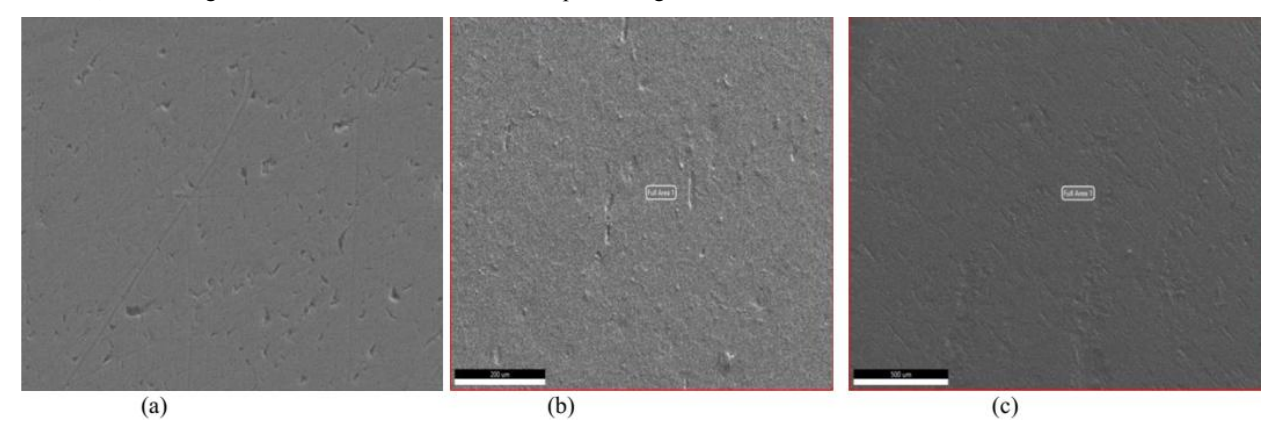


Figure 15: Scanning Electron Microscope of Monel 400 in 1M HCl a) without inhibitor b) 150 ppm Curcumin c) 200 ppm BCBAD

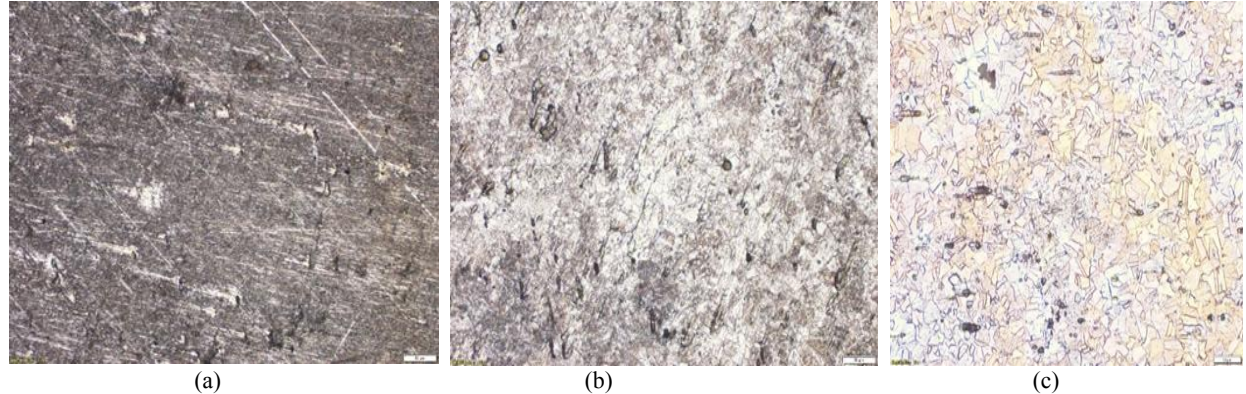


Figure 16: Microscope images of Monel 400 in 1M HCl by magnification 10x for (a) without inhibitor (b) 150 ppm Curcumin and (d) 200 ppm BCBAD

3.6.2. EXD

Figures 17 and 18 present comparative EDX spectra of 150 ppm curcumin and 200 ppm BCBAD. In the presence of inhibitors, Fig. 18, EDX spectra reveal a characteristic nitrogen peak. Concurrently, the carbon and oxygen signals show marked intensity

increases, suggesting enhanced surface coverage of organic species. The appearance of the nitrogen peak and the concurrent enhancement of carbon and oxygen signals directly correspond to the elemental composition of the inhibitor molecules. These spectral changes provide clear evidence of inhibitor adsorption on the metal surface, forming a protective layer. Data extracted from the spectra are presented in Tables 6,7. The EDX spectra reveal significant suppression of nickel signals in the presence of the inhibitor, indicating the formation of a dense surface film that attenuates the underlying metal substrate. This observation correlates well with electrochemical data, demonstrating that the protective film effectively [17,18].

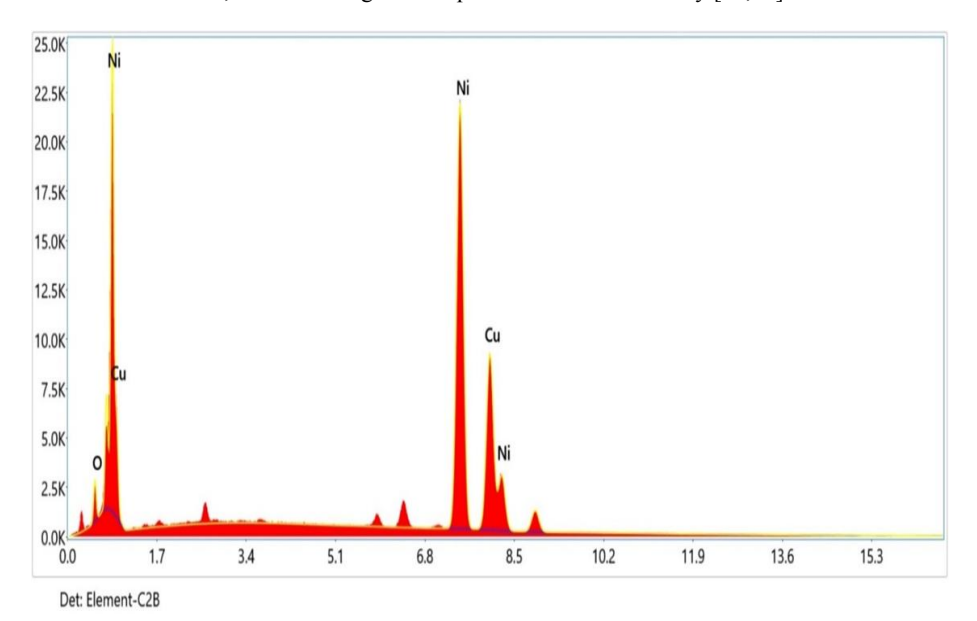


Figure 17: EXD of Monel 400 in 1M HCl for 150 ppm curcumin

Table 5: Data obtained from EDX of Monel 400 in 1M HCl for 150 ppm curcumin

Element	Weight %	Atomic %
OK	3.77	12.85
NiK	62.25	58.82
CuK	31.98	28.33

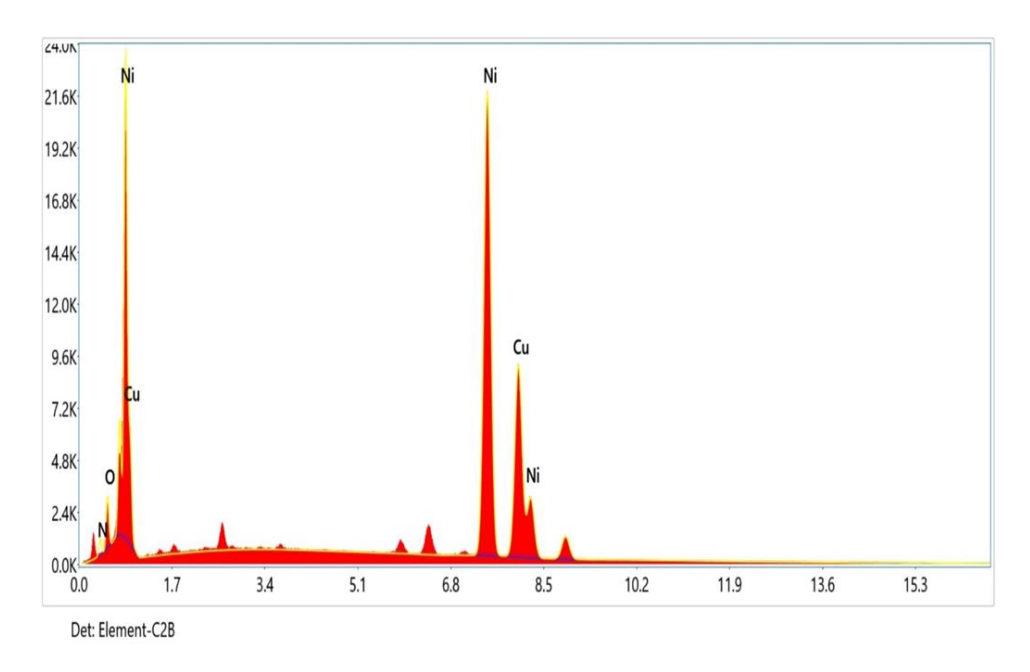


Figure 18: EDX of Monel 400 in 1M HCl for 200 ppm BCBAD

Table 6: Data obtained from EDX of Monel 400 in 1M HCl 200 ppm BCBAD

Element	Weight %	Atomic %
NK	2.89	10.18
O K	4.55	14.02
Ni K	60.01	51.13
Cu K	30.76	24.66

3.6.3. X-Ray Diffraction (XRD)

Figures 19,20 and 21 show the X-ray diffraction pattern for Blank, 150 ppm curcumin and 200 ppm BCBAD. In the presence of inhibitors, Fig. 20 and 21, Nickel oxide hydroxide Ni2O3H, copper hydroxide hydrate Cu(OH)₂.H₂O and Fig. 19 shows the presence of iron nitride (Fe₃ N) on the metal surfaces, which acts as a protective layer formed by the reaction between Monel and the inhibitor molecules. The high intensity of the corresponding peaks suggests that these compounds densely cover the metal surface, shielding the iron from corrosive agents. Additionally, the sharp narrow peaks indicate that the protective films exhibit a crystalline structure, enhancing their protective efficiency, this is further supported by the lack of corrosion products, confirming improved corrosion resistance in the presence of iron nitride [19]. Nitride coatings are widely used to enhance the hardness, wear resistance, and corrosion resistance of structural materials. They also find applications in high-tech industries where functional properties, rather than mechanical strength, are the key priority [20,21].

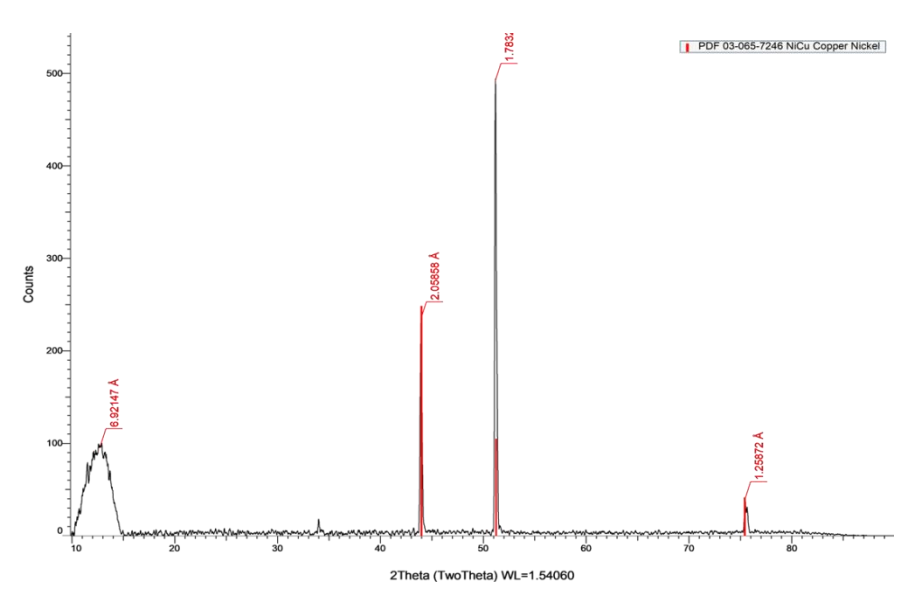


Figure 19: XRD of Monel 400 in 1M HCl for Blank

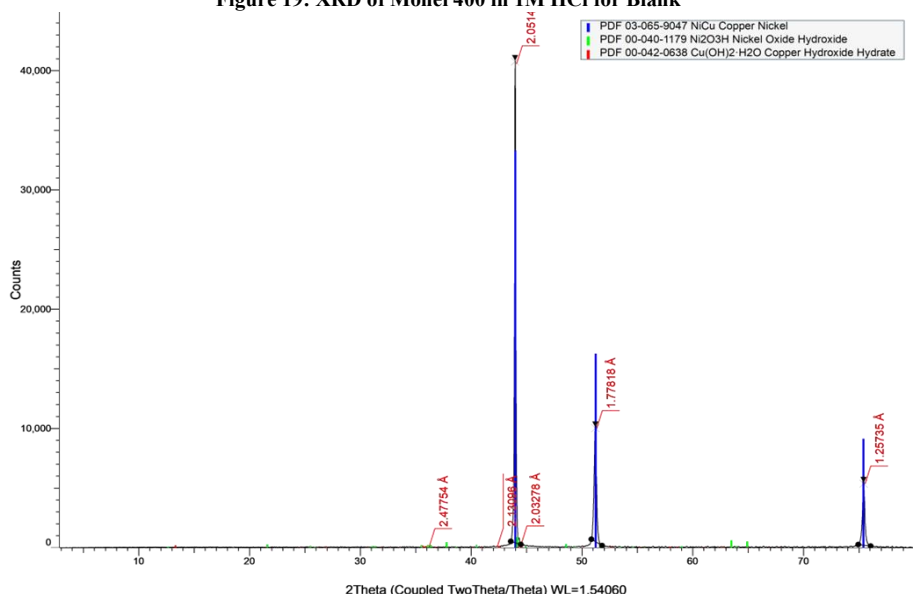


Figure 20: XRD of Monel 400 in 1M HCl for 150 ppm Curcumin

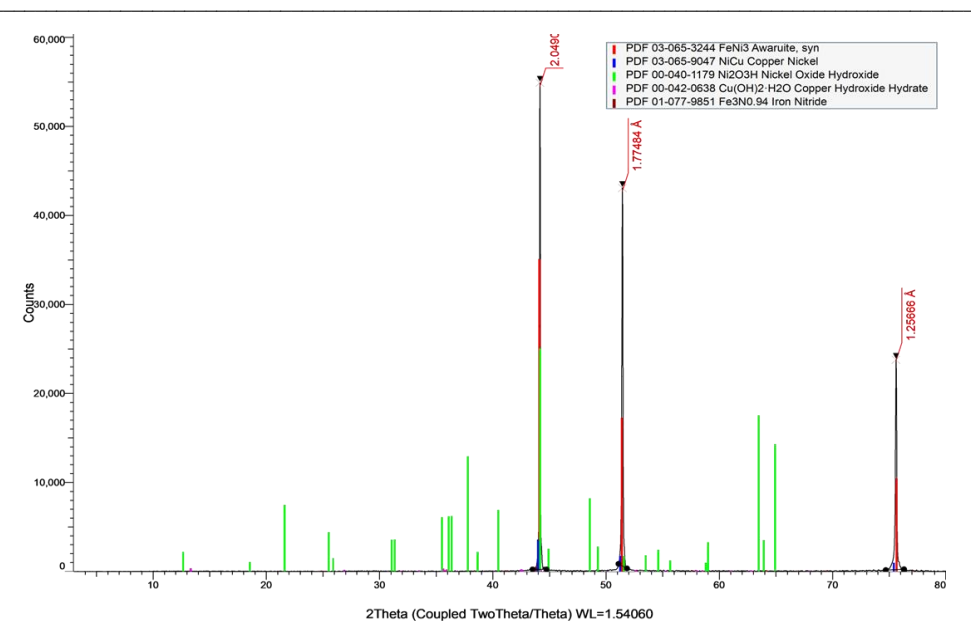


Figure 21: XRD of Monel 400 in 1M HCl for 200 ppm BCBAD

3.7 Mechanism of Corrosion Inhibition by BCBAD

3.7.1 Adsorption Process

Initial physisorption: BCBAD molecules are attracted to the Monel 400 surface via electrostatic interactions between protonated azo groups (-N=N-) and negatively charged metal sites (observed at OCP = -429 mV vs SCE).

Chemisorption: Coordinate bonds form through:

Electron donation from azo nitrogen lone pairs to vacant d-orbitals of Ni/Cu (confirmed by EDX: 2.89 wt% N)

Back-donation from metal to antibonding orbitals of C=O and -N=N- groups

3.7.2 Protective Layer Formation

Composition: XRD-identified Fe₂ N and CuO compounds (Fig. 21) create a 44.13 µm barrier (vs 27.33 µm for curcumin)

Morphology: SEM shows compact film with 3B adhesion (ASTM D3359) versus porous curcumin layer (1B)

3.7.3 Electrochemical Protection

Anodic inhibition: Blocks metal dissolution via:

 $Fe \rightarrow Fe^{2+} + 2e^{-}$ (suppressed by Fe_2 N formation)

 $Ni \rightarrow Ni^{2+} + 2e^{-}$ (prevented by Ni-azo complexes)

Cathodic inhibition: Reduces H^{\star} reduction by:

Occupying active Cu sites $(H^* + e^- \rightarrow \frac{1}{2}H_2)$

Increasing hydrogen overpotential ($\eta H = 125 \text{ mV}$).

3.7.4 Adsorption Mechanism Validation

FTIR: Shift in -N=N- stretch (1423 \rightarrow 1405 cm⁻¹) confirms metal coordination.

BCBAD's mixed inhibition outperform

The significance of these results lies in BCBAD's dual mechanism of action, involving both chemisorption and physisorption, which facilitates the formation of a stable barrier containing protective compounds like Fe₂ N and CuO. This work successfully establishes that molecular modification of natural compounds like curcumin is a powerful strategy for developing high-performance, environmentally benign corrosion inhibitors tailored for advanced industrial alloys under aggressive conditions.

3.7.5 Adsorption Behavior of BCBAD on Monel 400

Comparative Adsorption Capacity

Table 7: Comparative Adsorption Capacity

able 7. Comparative Musor priori Capacity					
Inhibitor Class	System	Efficiency (%)	Thickness (µm)	ΔG°ads (kJ/mol)	
Aloeferox extract	Cu/1 M HCl	93.3	5-10*	-38.2 (physisorption)	
Schiff base (III)	Carbon steel/1M HCl	93.0	_	-55.1	
Benzotriazole (BTA)	Monel 400/1 M HCl	91.5	15–20	-50.3	
BCBAD (This work)	Monel 400/1M HCl	94.8	44.13	-55.67	

4. Conclusions

The following conclusion could be derived from the above results:

- 4.1 Curcumin and BCBAD are good inhibitor applied to Monel 400 exposed to 1 M HCl. Moreover, all results indicate that the BCBAD compound exhibits a higher inhibition efficiency (94.84%) compared to Curcumin (75.72%), despite being less expensive. 4.2 The molecules of Curcumin and BCBAD adsorb onto the metal surface, forming a protective film that blocks active sites exposed to the corrosive medium. As the concentration of inhibitors increases, the corrosion rate decreases, reaching its minimum at 150 ppm for Curcumin and 200 ppm for BCBAD. However, further increases in the concentration of either inhibitor result in a rise in the corrosion rate.
- 4.3 SEM shows Scattered corrosion pits were observed on the Monel 400 surface exposed to 1 M HCl without inhibitor, less pits and no pits were observed on the Monel400 surface immersed in 1M HCl with 150 ppm of curcumin and 200 ppm BCBAD, respectively for 21 days at ambient temperature.
- 4.4 EDX spectra show the elemental analysis for the Monel 400 in 1M HCl with blank, 150 ppm of curcumin and 200 ppm of BCBAD. In case of curcumin Oxygen element peak was observed 3.77 % wt and BCBAD Nitrogen element peak was observed 2.89% wt. It is confirmed by these findings that the metal surface has been covered by a carbonaceous material containing these atoms. This layer is clearly attributed to the inhibitor. The results further indicate that the formation of this surface film has effectively reduced metal dissolution.
- 4.5 XRD analysis of the specimen surface in the presence of inhibited solutions reveals the formation of iron nitride and Fe₈ N), which indicates the development of a protective film resulting from the interaction between iron and the inhibitor molecules. (Fe₂ N

5. Conflicts of interest

The authors have no relevant financial or non-financial interests to disclose.

6. Formatting of funding sources

The author(s) received no financial support for the research.

7. Acknowledgments

All praise, thanks and indebtedness go to Allah who give me the easiness, the knowledge and the health to accomplish this work. I would like to thank and appreciate the man behind this work Prof. Dr. Eng. Mahmoud Ibrahim Abbas, from deep of my heart for his effort, helpful, supervision, reviewing and encouragement during all stages of the research till the end, also thank to Prof.Dr. Reda Mahmoud Abdel EL Aal for his great efforts, supervision, appreciate deeply to Assoc, helpful in practical stage, in publishing the paper and and advise. I would like to express my deepest gratitude to my Mother for her encouragement and support and greet thanks for my brothers.

8. References and Bibliography

- [1] Venterella, V. A.; Berretta, J. R.; de Rossi, W. Micro Welding of Ni-Based Alloy Monel 400 Thin Foil by Pulsed Nd:YAG Laser. Phys. Procedia 2011, *12*, 350–357.
- [2] Nasibi, M.; Mohammady, M.; Ashrafi, A.; Khalaji, A. A. D.; Moshrefifar, M.; Rafiee, E. Nanosized Scale Roughness and Corrosion Protection of Mild Steel in Hydrochloric Acid Solution and in the Presence of Turmeric (Curcuma longa) Extract as a Green Corrosion Inhibitor: FTIR, Polarization, EIS, SEM, EDS, AFM Studies, and Neural Network Modeling. J. Adhes. Sci. Technol. 2014, *28* (20), 2001–2015.
- [3] Shahba, R. M. A.; Fouda, A. E. E.; El-Shenawy, A. E.; Osman, A. S. M. Effect of Catharanthus roseus (Vince rosea) and Turmeric (Curcuma longa) Extracts as Green Corrosion Inhibitors for Mild Steel in 1 M HCl. Mater. Sci. Appl. 2016, *07* (10), 654–671.
- [4] Al-Fakih, A. M.; Aziz, M.; Sirat, H. M. Turmeric and Ginger as Green Inhibitors of Mild Steel Corrosion in Acidic Medium. J. Mater. Environ. Sci. 2015, *6*, 1480–1487.
- [5] Kherraf, S.; Zouaoui, E.; Medjram, M. S. Corrosion Inhibition of Monel 400 in Hydrochloric Solution by Some Green Leaves. Anti-Corros. Methods Mater. 2017, *64* (3), 347–354.
- [6] Verma, C.; Ebenso, E. E.; Bahadur, I.; Quraishi, M. A. An Overview on Plant Extracts as Environmental Sustainable and Green Corrosion Inhibitors for Metals and Alloys in Aggressive Corrosive Media. J. Mol. Liq. 2018, *266*, 577–590.
- [7] Elmorsi, M. A.; Hassanein, A. M. Corrosion Inhibition of Copper by Heterocyclic Compounds. Corros. Sci. 1999, *41* (12), 2337–2352.
- [8] Abdallah, M.; Moustafa, E. Inhibition of Acidic Corrosion of Carbon Steel by some Mono and Bis Azo Dyes Based on 1,5 Dihydroxynaphthalene. Ann. Chim. 2004, *94* (7-8), 601–611.
- [9] Alanazi, K. D.; Alshammari, B. H.; Alanazi, T. Y. A.; Alshammari, O. A. O.; Ashmawy, A. M.; Aljohani, M. M.; Haq, I.; Hameed, R. A.; Deyab, M. A. Thermodynamic, Chemical, and Electrochemical Studies of Aloe ferox Mill Extract as a Naturally Developing Copper Corrosion Inhibitor in HCl Solution. Sci. Rep. 2024, *14*, 11944.
- [10] Thabet, H. K.; AlGhamdi, J. M.; Mohamed, H. A.; Elsaid, M. A.; Ashmawy, A. M. Anticorrosion Agents for Carbon Steel in Acidic Environments: Synthesis and Quantum Chemical Analysis of New Schiff Based Compounds with Benzylidene. ACS Omega 2023, *8*, 39770–39782.
- [11] Ashmawy, A. M.; El-Sawy, A. M.; Khalil, H. F. Synthesis of Novel Liquid Crystal Compound and Study of its Behavior as Corrosion Inhibitor for Mild Steel in Acidic Medium 1 M HCl. Mol. Cryst. Liq. Cryst. 2022, *736* (1), [Article Number].

- [12] Abbas, M.; Ahmed, M. M. Z.; Abdel-Aleem, H. A.; Azab, N. Electrochemical Behavior of Dissimilar from Monel 400 and AISI 1020 Carbon Steel. Egypt. J. Chem. 2024, *67* (SI: M. R. Mahran), 1031–1036.
- [13] Mert, B. D.; Mert, M. E.; Kardas, G.; Yazıcı, B. Experimental and Theoretical Investigation of 3-Amino-1,2,4-triazole-5-thiol as a Corrosion Inhibitor for Carbon Steel in HCl Medium. Corros. Sci. 2011, *53* (12), 4265–4272.
- [14] Sanatkumar, B. S.; Nayak, J.; Shetty, A. N. Influence of 2-(4-Chlorophenyl)-2-oxoethyl Benzoate on the Hydrogen Evolution and Corrosion Inhibition of 18 Ni 250 Grade Weld Aged Maraging Steel in 1.0 M Sulfuric Acid Medium. Int. J. Hydrogen Energy 2012, *37*, 9431–9442.
- [15] Okafor, P. C.; Liu, X.; Zheng, Y. G. Corrosion Inhibition of Mild Steel by Ethylamino Imidazoline Derivative in CO₂ -Saturated Solution. Corros. Sci. 2009, *51* (4), 761-768.
- [16] Heydari, M.; Javidi, M. Corrosion Inhibition and Adsorption Behavior of an Amido-imidazoline Derivative on API 5L X52 Steel in CO₂ -Saturated Solution and Synergistic Effect of Iodide Ions. Corros. Sci. 2012, *61*, 148–155.
- [17] Li, W. H.; He, Q.; Zhang, S. T.; Pei, C. L.; Hou, B. R. Some New Triazole Derivatives as Inhibitors for Mild Steel Corrosion in Acidic Medium. J. Appl. Electrochem. 2008, *38* (3), 289–295.
- [18] Rehim, S. S. A.; Hazzazi, O. A.; Amin, M. A.; Khaled, K. F. On the Corrosion Inhibition of Low Carbon Steel in Concentrated Sulphuric Acid Solutions. Part I: Chemical and Electrochemical (AC and DC) Studies. Corros. Sci. 2008, *50* (8), 2258–2271.
- [19] Fragoza-Mar, L.; Olivares-Xometl, O.; Domínguez-Aguilar, M. A.; Flores, E. A.; Arellanes-Lozada, P.; Jiménez-Cruz, F. Corrosion Inhibitor Activity of 1,3-Diketone Malonates for Mild Steel in Aqueous Hydrochloric Acid Solution. Corros. Sci. 2012, *61*, 171–184.
- [20] Prev'ey, P. S. X-ray Diffraction Characterization of Crystallinity and Phase Composition in Plasma-Sprayed Hydroxyapatite Coatings. J. Therm. Spray Technol. 2000, *9* (3), 369–376.
- [21] Bertóti, I. Characterization of Nitride Coatings by XPS. Surf. Coat. Technol. 2002, *151-152*, 194-203.